



Experimental characterization of the quasi-static and dynamic piezoresistive behavior of multi-walled carbon nanotubes/elastomer composites

Nicolas Penvern, André Langlet, Michel Gratton, Marcel Mansion, Nourredine Aït Hocine

► To cite this version:

Nicolas Penvern, André Langlet, Michel Gratton, Marcel Mansion, Nourredine Aït Hocine. Experimental characterization of the quasi-static and dynamic piezoresistive behavior of multi-walled carbon nanotubes/elastomer composites. *Journal of Reinforced Plastics and Composites*, 2020, 10.1177/0731684420901754 . hal-02563617

HAL Id: hal-02563617

<https://hal.science/hal-02563617>

Submitted on 5 May 2020

HAL is a multi-disciplinary open access archive for the deposit and dissemination of scientific research documents, whether they are published or not. The documents may come from teaching and research institutions in France or abroad, or from public or private research centers.

L'archive ouverte pluridisciplinaire **HAL**, est destinée au dépôt et à la diffusion de documents scientifiques de niveau recherche, publiés ou non, émanant des établissements d'enseignement et de recherche français ou étrangers, des laboratoires publics ou privés.

Experimental characterization of the quasi-static and dynamic piezoresistive behavior of multi-walled carbon nanotubes/elastomer composites

Nicolas Penvern¹, André Langlet¹ , Michel Gratton²,
Marcel Mansion³ and Nourredine Aït Hocine²

Abstract

Multi-walled carbon nanotube (MWCNT)/elastomer composites exhibit a piezoresistive behavior, i.e. their resistivity changes when they are subjected to mechanical loading. Thus, these materials can be used as strain or pressure sensors. In this paper, the effect of carbon nanotube weight fraction on the sensitivity and repeatability of the electrical response of multi-walled carbon nanotube/ethylene–propylene–diene monomer composites is investigated, under quasi-static and dynamic compression (using split Hopkinson pressure bars). It was found that multi-walled carbon nanotube weight fraction and the strain rate have a major influence on the piezoresistivity of such composites. Although all samples exhibited a good repeatability of their electrical response under quasi-static cyclic compression, those with a lower multi-walled carbon nanotube weight fraction had a higher sensitivity to strain. An increase in the electrical resistance during compression was observed under both quasi-static and dynamic compression. Reversible movements of multi-walled carbon nanotube in the transverse direction of compression increased the average inter-multi-walled carbon nanotube distance under quasi-static compression, leading to higher values of resistance. After the dynamic tests, the Young's modulus of the composites decreased by about 45% and the electrical resistance increased a hundredfold, indicating damage induced by dynamic loading.

Keywords


Piezoresistivity, carbon nanotubes, elastomer, split Hopkinson pressure bar loading, quasi-static compression

Introduction

Carbon nanotube (CNT) elastomer composites have attracted scientific interest because of their high compliance and their significantly improved electrical properties.^{1–4} CNT can form a continuous conductive network inside elastomers even at a very low weight fraction, characterized by a sharp increase in the electrical conductivity and well known as the percolation threshold. The percolation threshold corresponds to the CNT volume fraction at which the composite exhibits a structured three-dimensional (3D) network and it is moved from an electrically insulative state to an electrically conductive state. When these materials are subjected to mechanical loading, the conductive network can change in many ways, leading to a modification of the electrical resistance. Thus, CNT/elastomer nanocomposites can be used in industry,

for instance, for strain sensing^{3,5,6} or damage localization inside structures.^{7,8}

Obtaining a homogeneous dispersion of CNTs inside elastomer matrices is of major importance to ensure high mechanical reinforcement and a 3D electrically conductive network. In fact, CNTs tend to agglomerate because of high Van der Waals

 Laboratoire Gabriel LaMé, Univ. Orléans, Univ. Tours, INSA CVL, 18000 Bourges, France

²Laboratoire Gabriel LaMé, INSA CVL, Univ. Tours, Univ. Orléans, France

³ATCOM Télémetrie, Chécy, France

Corresponding author:

André Langlet, Laboratoire Gabriel LaMé, Univ. Orléans, Univ. Tours, INSA CVL, 63 Av. de Lattre de Tassigny, 18000 Bourges, France.
Email: Andre.Langlet@univ-orleans.fr

interactions between their walls. Huang and Teretjev⁹ have studied, in terms of energy density, the ability to break CNT aggregates without breaking the individual CNTs, by transferring local shear stresses to the polymer/CNT blend through rotor movements, during mechanical shear mixing, or through particles agitation provided by ultrasonication. Mechanical shear mixing is well suited to homogeneously disperse CNTs inside elastomers, because it can break the CNT aggregates but not the individual CNTs.¹

As explained in the work of Gong and Zhu,¹⁰ the change in electrical resistance under strain, known as the piezoresistivity, is governed by two mechanisms:

- Electron tunneling between two CNT junctions: electrons can go through the insulating elastomer from one CNT to another. The insulating polymer that separates two adjacent CNT is called the tunneling film. It is commonly assumed that tunneling occurs when the thickness of the tunneling film is less than 1.4 nm. The thinner the tunneling film, the lower the tunneling resistance.
- Under compression, CNT tunneling junctions may slide, leading to the separation between CNTs.

Most of the literature studies deal with the characterization of the piezoresistive behavior of CNT/elastomer composites under quasi-static tension or compression.

Ciselli et al.⁵ and Costa et al.⁶ analyzed the increase in the electrical resistance of CNT/elastomer composites under tensile loading, by increasing the distance between CNTs until their separation. In this case, electron tunneling is the main piezoresistive mechanism involved.

When a compressive force is applied to the composites, their electrical behavior depends on the interactions between the CNTs and the elastomer macromolecules, the amount of CNTs added to the elastomer and the dispersion degree of these particles. It is worth noting that the higher the dispersion degree of the particles in the matrix, the more homogeneous the microstructure of the composite. The strain rate and the maximum strain reached during the tests also play a key role in the piezoresistivity behavior of such composites.

Ku-Herrera and Aviles¹¹ studied the piezoresistive behavior of vinyl-ester/0.3 wt.% multi-walled carbon nanotube (MWCNT) composites under quasi-static cyclic axial tension and compression. The electrical resistance showed a reversible behavior (increasing during tension then decreasing during unloading). They revealed that, because of the viscoelasticity of the matrix, the amplitude of the resistance between consecutive cycles decreases slightly. Similar behavior was

observed by Costa et al.⁶ with styrene-butadiene-styrene/MWCNT composites. When the composites were subjected to quasi-static compression, their electrical response in the elastic and plastic regions differed. In the elastic region (compressive strain below 3%), the resistance decreased slightly because of the rearrangements of the MWCNT inside the matrix. In the plastic region, the electrical resistance of the composite increased due to the sliding of the MWCNT junctions. Thus, they showed that the MWCNT network is sensitive to matrix yielding and plastic strain level.

The capability of CNT composite films to be used as strain or pressure sensors was fully studied by Wang et al.^{12,13} They analyzed the piezoresistivity of silicone/MWCNT composites during quasi-static compression.¹² The amount of MWCNT used in their composites was in the range of 4 to 12 wt.%. When the weight fraction of CNT was lower than 6%, they found that the electrical resistance of the composites increased monotonically with increasing pressure, making it possible to infer the stress from the measured resistance. Over 6 wt.%, they observed that the resistance increased slightly at the beginning of the compression (stress below 0.1 MPa) and then decreased sharply over 0.1 MPa. Wang et al.¹³ used the same method to deduce the strain from the electrical response to compression of epoxy/CNT film composites. The increased resistance was also analyzed regarding the Young's modulus of the matrix. When the Young's modulus of the matrix was increased, more stress was transferred to the CNT network and thus, the CNTs followed the movements of the epoxy. Thus, the CNTs orientate in the transverse direction of the mechanical loading, leading to fewer contacts in the conductive network and higher electrical resistance. Similar results were obtained in the studies by Hao et al.,¹⁴ Mitrakos¹⁵ and Spinelli et al.³

An interesting work published by Zha et al.¹⁶ investigated the influence of adding carbon black (CB) on the electrical response during quasi-static compression of a silicone/CNT composite. Adding CB helps to obtain a homogeneous dispersion of MWCNT inside the matrix, as CB particles act as bonding between the MWCNT and the ethylene-propylene-diene monomer (EPDM) macromolecules.¹⁶ However, the presence of CB causes the CNTs to orientate in the transverse direction of the compression, leading to fewer contacts between CNTs and thus increasing electrical resistance.

The electrical response of polymer/MWCNT composites under dynamic compression has been investigated in only a few studies. Heeder et al.² studied the electrical response of an epoxy/MWCNT composite under split Hopkinson pressure bar (SHPB) loading and drop-weight impact. Their investigations revealed an increase in the electrical resistance during dynamic

compression, caused by delamination at the interphase between epoxy and the MWCNT, due to poor bonding. In their work, Baltopoulos et al.⁷ exploited the capability of the MWCNT network to detect and localize damage (such as holes or oblong notches) inside epoxy/MWCNT composites. Local damage was then revealed by a local decrease in the electrical conductivity near the damage. Gao et al.⁸ also used the CNT network inside a woven glass fabric for in situ damage detection. The electrical resistance increased during repeated drop-weight impact loading, associated with intra-bundle cracking and delamination.

Although MWCNT networks have shown their potential to detect damage inside polymer composites, there is still limited knowledge how the electrical response varies with strain rate, and especially during SHPB compression and unloading. This study presents analyses of the electrical response of composites made of an EPDM matrix reinforced by both CB and MWCNT, under quasi-static compression and SHPB loading. By using a short striker, the electrical response during dynamic unloading could be captured, which constitutes a major advance in the study of the piezoresistive behavior of such composites during dynamic loading. A method to assess the damage induced by dynamic loading is proposed. This method is based on the comparison of the mechanical behavior and electrical response of the EPDM/5% MWCNT composite over a quasi-static compressive cycle before and after the SHPB test.

Materials and methods

Materials and samples

The studied composites are made of an EPDM matrix, CB obtained by the fast extraction furnace process and MWCNT produced by Arkema using chemical vapor deposition. The number of walls of the MWCNT is between 5 and 15. They are 0.1–10 μm long and their outer diameter is between 10 and 15 nm, leading to an aspect ratio (length over diameter) of about 1000. The MWCNT were initially in the form of spherical aggregates with a diameter of 200 to 500 μm .

CB of 25 wt.% was added to the EPDM matrix. The MWCNT weight fractions used were 0, 1, 3 and 5%. Cylindrical samples of 16 mm length and 20 mm diameter, cross-sectional area were obtained by shear mixing of all the compounds.

Two cylindrical brass electrodes are placed in the top and bottom surfaces of the samples in order to measure the electrical resistance of the composites. As shown in Figure 1, the electrodes are 3 mm thick and their diameter is 20 mm. Thus, the effective length of the composite, denoted as L_0 hereinafter, is 10 mm.

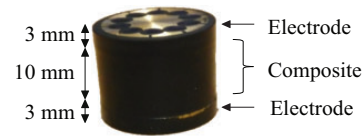


Figure 1. An overmolded sample with brass electrodes.

Table 1. Composition and number of tested samples.

Denomination	% CB	% CNT	Number of samples
EPDM/0% CNT	25	0	2
EPDM/1% CNT	25	1	2
EPDM/3% CNT	25	3	2
EPDM/5% CNT	25	5	3

EPDM: ethylene–propylene–diene monomer; CNT: carbon nanotube.

In order to achieve an optimal mechanical contact between the brass electrodes and the composites, the electrodes are inserted in the top and bottom plane surfaces of the cylindrical mold. The composite is assembled with the brass electrodes during the reticulation phase. This process is called “overmolding”. A view of an overmolded sample is shown in Figure 1.

The composition of the tested samples and the number of samples for each condition is given in Table 1.

Measurement of the electrical impedance

To measure the electrical impedance of the samples, brass electrodes are placed in contact with the opposite plane surfaces of the cylindrical samples, as shown in Figure 1. The electrical response of the sample is characterized by imposing an electrical current intensity I (input variable) through the linear measurement device, whose electronic scheme is shown in Figure 2. The current I is ranging from 10 μA to 3 mA. The amplifier of the device has high impedance and unit gain, acting as a current amplifier while having the same input and output voltage V . The slew rate of the ohmmeter is 10 V/ μs , allowing a fast response of the measurement device to mechanical external loading. The electrodes are connected to the device with low-capacity coaxial wires. The voltage at the terminals of the sample is obtained as an output variable of the measurement device. The saturation voltage of the device is equal to 4.5 V. Thus, the range of measurement of the device can be adjusted by choosing an appropriate current. The ratio between the output voltage V and the input intensity I characterizes the electrical impedance of the sample denoted Z in the following. The impedance has the same dimension as an electrical resistance.

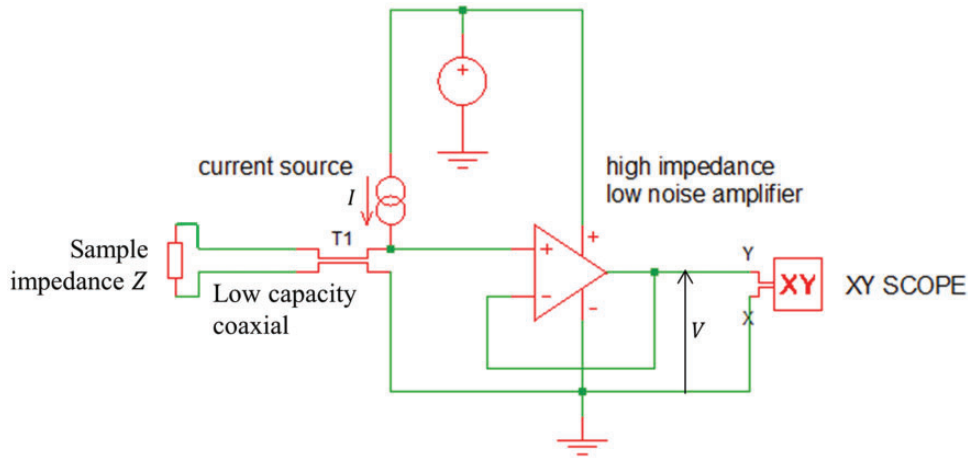


Figure 2. Ohmmeter used to measure the electrical resistance.

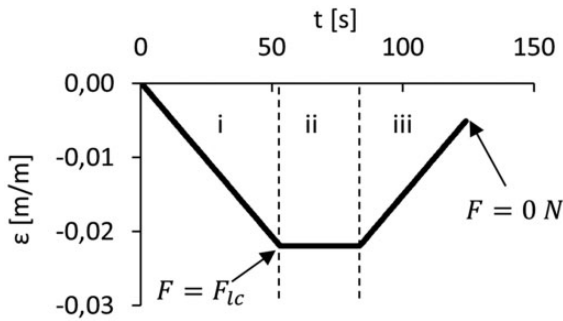


Figure 3. Procedure used for quasi-static cyclic compression tests.

Characterization of the material piezoresistivity under quasi-static loading

Monotonic and cyclic compression tests were carried out on all samples, and the electrical impedances of these samples were measured during the test.

As shown in Figure 3, the cyclic compression tests, of about 2 min, consist of:

- A compression, with a displacement speed v equal to 0.25 mm/min, corresponding to the strain rate $\dot{\epsilon}$ of $4.1610^{-4} \text{s}^{-1}$. The compression is stopped when the force reaches F_{lc} . This force is chosen so that the electrical resistance remains below 450 k Ω during the test. For the EPDM/0% MWCNT composite, F_{lc} is equal to -100 N. For the other samples, F_{lc} is set to -200 N, for the same reasons.
- A relaxation of 30 s. This duration is chosen to obtain stabilized values of the electrical impedance of the samples.
- An unloading with a displacement speed of 0.25 mm/min, until the force reaches 0 N. At the

end of the compression cycle, a residual strain remains, because of the viscoelasticity of the matrix.

In order to compare the mechanical and electrical behavior before and after the dynamic tests, low amplitudes of force were chosen to carry out the compression, so that the samples do not suffer damage during the quasi-static (QS) tests.

The electrical response of the undamaged composites under repeated cyclic compression was studied during 50 cycles of loading (step 1) and unloading (step 3). During these tests, the strain level of the composites was below 5%.

The tests were done using an MTS tension compression machine equipped with a load cell of 10 kN, and controlled with a computer using TWE Elite software (Figure 4(a)). An alignment device divided into two parts (in contact through a grease film) and containing a notch to place the sample was used so that the sample is subjected to pure uniaxial compression (Figure 4(b)). The sample is electrically insulated from the heads, thanks to an adhesive.

The nominal strain ϵ is assessed through the displacement u of the upper crosshead

$$\epsilon = \frac{u}{L_0} \quad (1)$$

where L_0 is the initial effective length of the sample.

The electrical sensitivity of the samples is evaluated through their gage factor, defined as follows

$$GF = \frac{\Delta Z}{Z_0} \frac{1}{\Delta \epsilon} = \frac{Z - Z_0}{Z_0} \frac{1}{\epsilon - \epsilon_0} \quad (2)$$

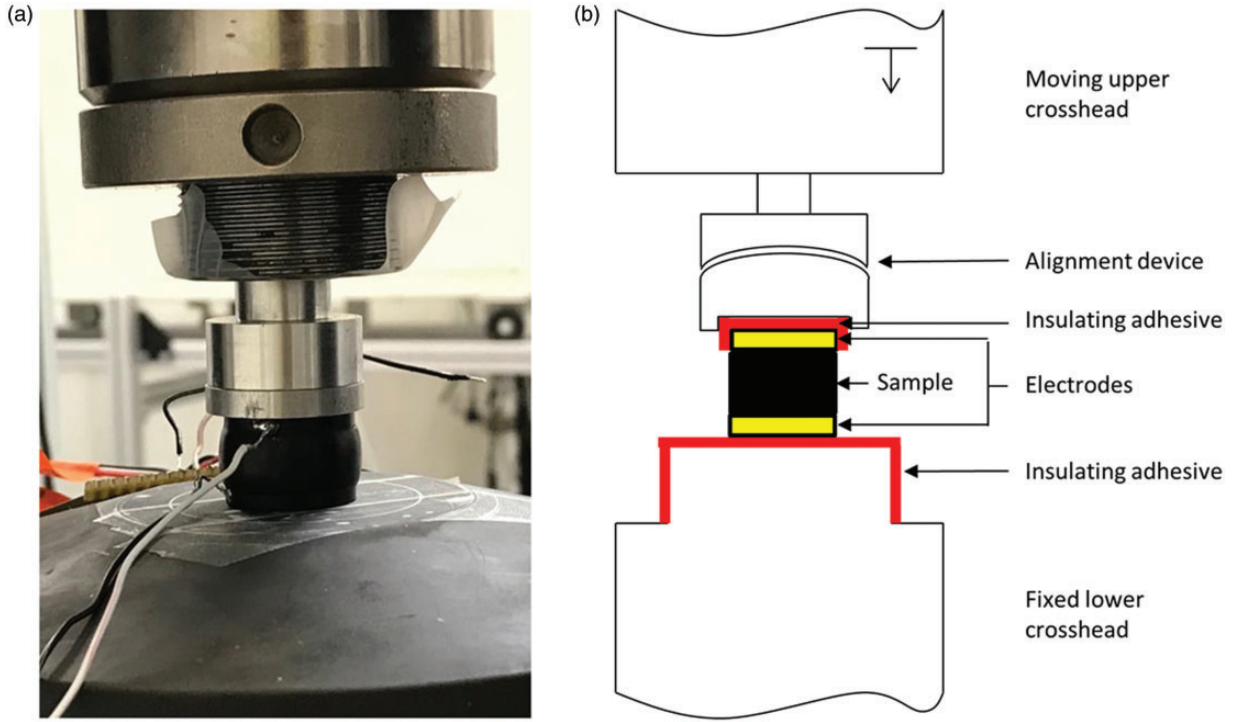


Figure 4. (a) Compression test of an EPDM/MWCNT sample. (b) Scheme of the alignment device.

where Z and Z_0 are the electrical impedances corresponding to the applied strains ε and ε_0 , respectively. ε_0 is zero at the beginning of monotonic and cyclic compressive tests.

The higher the gage factor, the higher the electrical sensitivity of the composites to strain.

Characterization of the material piezoresistivity under SHPB loading

The mechanical behavior of the composites at high strain rates was investigated using a SHPB apparatus composed of three main parts: the input bar (IB), of length 3 m, the output bar (OB, 1.75 m long) and the striker (0.5 m length). The specimen is placed between the two bars. The diameter of the bars, equal to 20 mm, is very small compared with their respective length. Thus, the waves propagate unidirectionally inside the bars.

On the IB, gage 1 measures the incident and reflected strains ε_i and ε_r . On the OB, gage 2 measures the transmitted strain ε_t at 0.4 m from the interface **O**. To measure distinctly the incident and reflective waves, gage 1 on the IB is bounded at 1.5 m from the interface **I** (Figure 5). The signals are then conditioned, amplified and visualized using Labview[®].

The whole test is filmed by a fast camera, with a frame rate of 100,000 images per second. A schematic view of the SHPB apparatus is given in Figure 5.

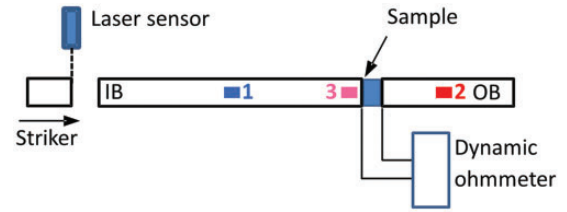


Figure 5. Schematic view of a SHPB apparatus.

When the striker hits the IB, a longitudinal incident wave propagates inside the IB. A part of the incident wave is transmitted to the OB through the sample. During the test, the wave propagates in the sample: it corresponds to a transient phase during which the stress state is not uniform. The dynamic equilibrium phase is reached when the stress is uniform over the sample.

The reflection and transmission coefficients at the interface between the IB and the sample, respectively, denoted as RC and TC are given by the following equations

$$RC = \frac{Z_B - Z_S}{Z_B + Z_S} \quad (3)$$

$$TC = \frac{2Z_S}{Z_B + Z_S} \quad (4)$$

Table 2. Properties of EPDM sample and nylon bars.

Material	E (Pa)	ρ (kg/m ³)
Nylon	3.3×10^9	1200
EPDM	50×10^6	1150

EPDM: ethylene-propylene-diene monomer.

where Z_S and Z_B are the mechanical impedances of the sample and the bar, respectively. The mechanical impedance of the bar Z_B is given by equation (5).

$$Z_B = S_B \sqrt{E_B \rho_B} \quad (5)$$

In equation (5), S_B is the cross-section of the bar, E_B is the Young's modulus of the bar and ρ_B is the density of the bar. The impedance of the sample is defined using the same equation. The properties of the bar and the samples are given in Table 2.

Nylon bars were used to carry out the dynamic tests because the values of RC (0.785) and TC (0.215) obtained from equations (3) to (5) lead to exploitable measured strains.

A key point during the analysis of the results of the SHPB tests is the synchronization between the mechanical variables (equations (6) to (12)) and the electrical impedance. When the laser velocity sensor detects the striker just before it hits the IB, the total measurement chain and the camera are triggered with time t' . The wave front arriving at interface **I** is detected by gage 3 at time t'_0 (graph on the top of Figure 6).

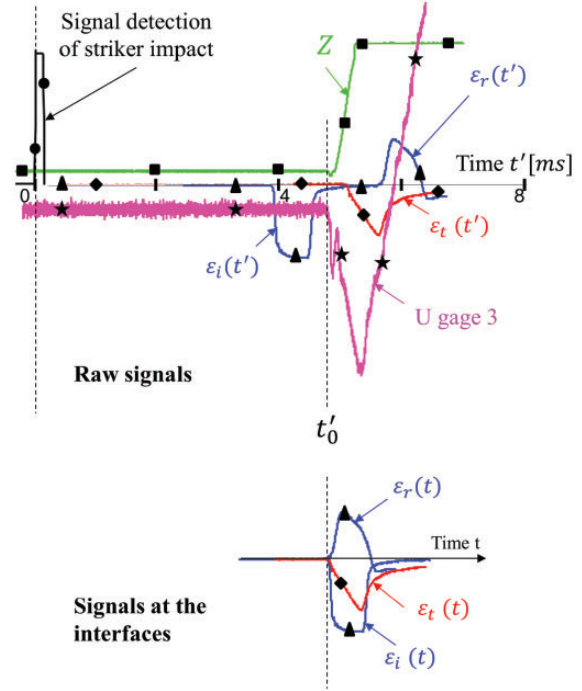
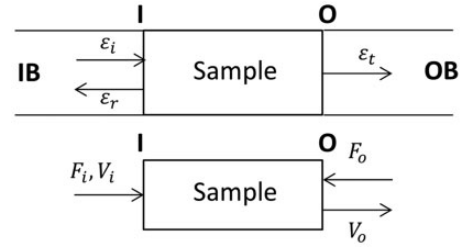
The strain signals must be known at the interfaces **I** and **O**, although being measured at distant positions from the interfaces. The algorithm of Gary and Zhao¹⁷ was used to infer the values at the interfaces from their measurements at the positions **1** and **2** (graph on the bottom of Figure 6). This algorithm is based on the wave velocities and dispersion equations in the linear visco-elastic nylon bar to shift the strain waves from their respective measurement locations to the interfaces. After this procedure, the forces F_i and F_o and velocities V_i and V_o , respectively, at interfaces **I** and **O** (Figure 7), as well as the strain, stress and strain rate of the sample are deduced by equations (6) to (12)

$$F_i(t) = E_B S_B (\varepsilon_i + \varepsilon_r) \quad (6)$$

$$F_o(t) = E_B S_B \varepsilon_t \quad (7)$$

$$V_i(t) = -c_B (\varepsilon_i - \varepsilon_r) \quad (8)$$

$$V_o(t) = -c_B \varepsilon_t \quad (9)$$

**Figure 6.** Raw signals measured during the SHPB test of an EPDM/1% MWCNT composite; signals transported at interfaces.**Figure 7.** Waves, forces and velocities at the input “I” and output “O” interfaces.

$$\dot{\varepsilon}(t) = \frac{V_i - V_o}{L_0} \quad (10)$$

$$\varepsilon(t) = \int_0^t \dot{\varepsilon}(t) dt \quad (11)$$

$$\sigma_m(t) = \frac{F_i + F_o}{2S_E} \quad (12)$$

where t is the time base of the transported signals (Figure 6).

It is well known in SHPB testing that force F_i begins to rise before F_o . A dynamic equilibrium state takes place when F_i is equal to F_o . Consequently, the stress state is then homogeneous in the sample and assumed equal to σ_m . In the present study, the duration

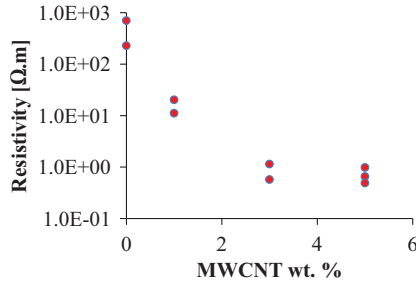


Figure 8. Change in resistivity of the EPDM/CB/MWCNT composites vs. the MWCNT weight fraction.

of the compressive incident crenel ε_i is adjusted so that the forces F_i and F_o start to decrease while being still equal. Thus, the dynamic unloading of the samples can be measured.

Results and discussion

Initial electrical resistivities of the EPDM/MWCNT composites

In Figure 8, the resistivity vs. the weight fraction of the unloaded EPDM/CB/MWCNT composites is plotted.

All composites are conductive, even when there are no CNTs inside. This result comes from the high CB weight fraction (25%) dispersed inside the matrix. Similar measurements were done by Ciselli et al. on rectangular samples containing EPDM and MWCNT only.⁵ The electrical resistivity of their 3 wt.% MWCNT composites was equal to $10^9 \Omega.m$.⁵ By adding 25 wt.% of CB in our composites, the electrical resistivity of our composites is far lower.

The values of electrical resistivity of the composites having the same MWCNT weight fraction are close. This observation confirms the reliability of the process used to manufacture the sample.

When the MWCNT weight fraction becomes higher than 3%, there is not a significant improvement of the initial electrical properties of the composite. This indicates that the conductive network, composed by CB and MWCNT, becomes saturated at such filler concentrations.

Electrical response of composites under quasi-static tests

Compressive cycle. The changes of strain and electrical impedance over time of two similar EPDM/5% MWCNT composites under a QS compressive cycle are plotted in Figure 9.

Although the results present experimental discrepancies, the curves exhibit similar trends. Indeed, for both samples, the resistance decreases at the beginning

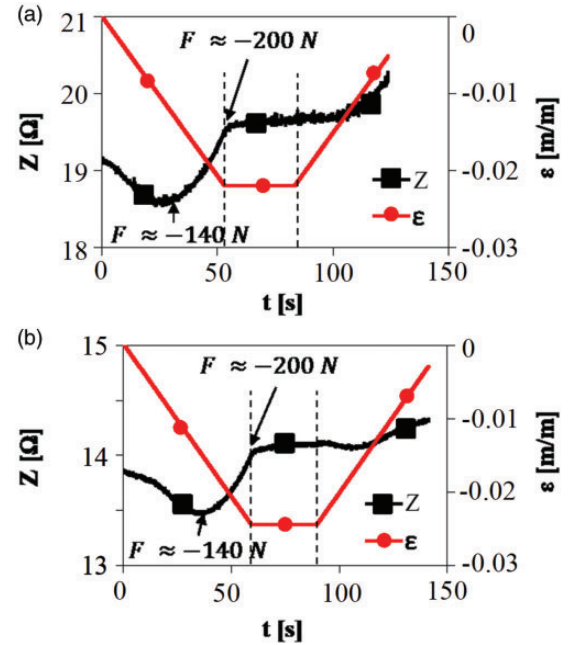


Figure 9. Change of strain and electrical impedance during one compressive cycle of two similar EPDM/5% MWCNT composites (a) and (b).

of the compression and then increases once the absolute value of the force becomes greater than $-140 N$. The decrease in the electrical resistance at the beginning of the compression can be attributed to the decrease of the distances between MWCNT, leading to a decrease in the tunneling resistance and formation of new contacts between MWCNTs. Thus, the electrical impedance decreases during this phase.

When the absolute value of the force becomes high enough, the MWCNT network reorientates in the transverse direction of the compression loading. Thus, sliding occurs between MWCNT particles and separates them, leading to an increase in the resistance. According to the work of Zha et al.,¹⁶ the presence of CB at weight fraction higher than 3% inside the composite emphasizes the reorientation of MWCNT and thus the sliding phenomenon. The resulting losses of conductive paths inside the matrix are revealed by the variations of the electrical impedance. This result is similar to those obtained by Hao et al.,¹⁴ Ku-Herrera and Aviles,¹¹ Mitrakos,¹⁵ Spinelli et al.³ and Wang et al.^{12,13}

During stress relaxation, the strain of the specimen is kept constant. The electrical resistance of the composites during stress relaxation does not change significantly, suggesting minor modifications of the microstructure of the conductive network formed by CB and MWCNT.

The electrical behavior during unloading is not symmetrical to the one during compression. This result

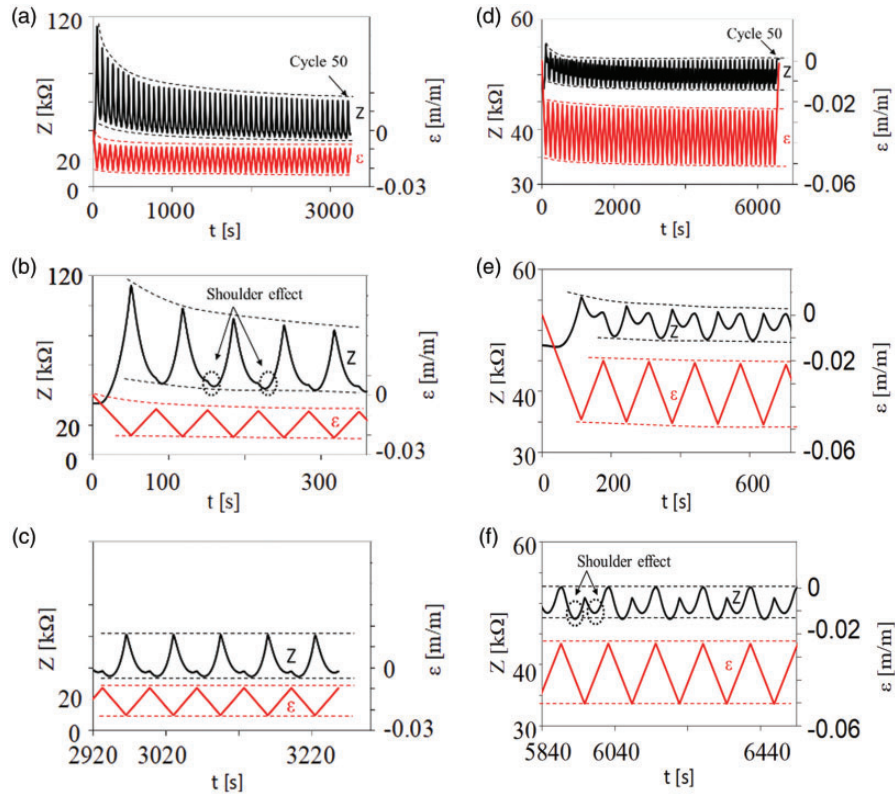


Figure 10. Changes of the electrical impedance and strain of the composites EPDM/0% MWCNT (a–c) and EPDM/3% MWCNT (d–f) during 50 compression cycles: all cycles (a,d); cycles 1–5 (b,e); cycles 46–50 (c,f).

may be explained by weak bonding between the MWCNT and the elastomer chains. In this case, the stress is not properly transferred from the matrix to the conductive network, leading to minor modifications of the conductive network.

Piezoresistive behavior of EPDM/MWCNT composites under QS cyclic compression. Cyclic compression tests were carried out on the samples containing 0 and 3 wt.% of MWCNT, as described in the “Characterization of the material piezoresistivity under quasi-static loading” section. The compression tests consisted of 50 cycles of saw teeth compression loading and unloading, without a relaxation step (Figure 10(b) and (c)). Two samples with the same MWCNT weight fraction were characterized.

The change in impedance and strain of the samples EPDM/0% MWCNT and EPDM/3% MWCNT over time is given in Figure 10. A zoom is made on the first (Figure 10(b) and (e)) and last five cycles (Figure 10(c) and (f)) of each test.

The amplitude of impedance response of the composites decrease initially and then stabilize with increasing time (Figure 10(c) and (f)). The upper and lower envelopes of the strain and the impedance are plotted in dashed lines. This behavior is certainly related to the

accommodation of the composites under cyclic loading. From a mechanical point of view, as the same force is applied at the end of the compression for each cycle, stress-softening of the matrix occurs, leading to an increase in the absolute maximum value of the strain between each cycle (Figure 10(a) and (d)).

The electrical response of the EPDM/3% MWCNT shows a decrease trend followed by an increase at the beginning of each compression cycle (Figure 10(b) and (c)), known as the “shoulder effect”. Although the origin of this effect is not clearly understood, it is often associated with the orientation of the CB or CNT particles.³

Sensitivity of the composites under monotonic QS compression. To study the effect of the MWCNT weight fraction on the electrical sensitivity of the composites, uniaxial compression tests were carried out on these composites, with a displacement speed of 0.25 mm/min. For all materials, the tests were conducted until saturation of the electrical measurement device. Using the definition of the gage factor, given by equation (2), the sensitivity of the composites can be evaluated by plotting the normalized change of impedance $\Delta Z/Z_0$ with respect to strain ε . The curves obtained are shown in Figure 11. As the piezoresistive

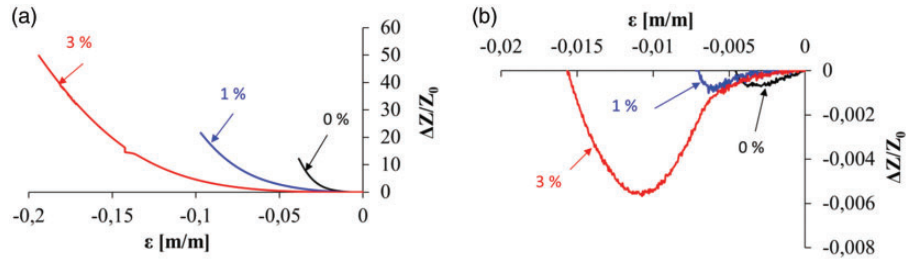


Figure 11. Normalized change in composite electrical impedance with respect to strain: (a) during the whole test; (b) zoom on the strains below 2%.

behavior is different for strains below 2%, a zoom has been done on the curve (Figure 11(b)). As stated in the “Electrical response of composites under quasi-static tests” section, the impedance of the composites slightly decreases at small strains, and then dramatically increases. At low strains, CNT particles are getting closer during compression, leading to a decrease in the average distance between them, and thus a decrease in the resistance by tunneling effect. At higher strain, the reorientation of CNT at the transverse direction causes the separation of CNT and thus to an increase in the electrical resistance. The lower the MWCNT weight fraction, the higher the sensitivity of the samples to strain. In fact, as the MWCNT wt.% increases, a more structured conductive network is formed inside the elastomer. Thus, when a small compression is applied to the composite, minor changes in the conductive network will occur, leading to a lower change in the impedance and thus to the sensitivity of the composite.

SHPB compressive tests

Dynamic behavior of the EPDM/MWCNT samples. SHPB experiments were carried out on the EPDM/MWCNT samples containing between 0 and 5 wt.% of MWCNT, using a short striker of 0.5 m length. The striker is launched using an air gun with a speed of about 17 m/s, inducing a sample strain rate of 700 s^{-1} , during the compression loading, and -400 s^{-1} , during the unloading. Using the procedure explained in the “Characterization of the material piezoresistivity under SHPB loading” section, the dynamic stress-strain and impedance-strain curves are plotted in Figure 12.

There is not a significant influence of the MWCNT weight fraction on the mechanical behavior of the over-molded composites under impact loading (Figure 12 (a)). This can be attributed to the weak interactions between the polymer and the MWCNT, and to the high amount of CB dispersed inside the matrix.

As the resistance of the composites containing between 0 and 3 wt.% of MWCNT increases very

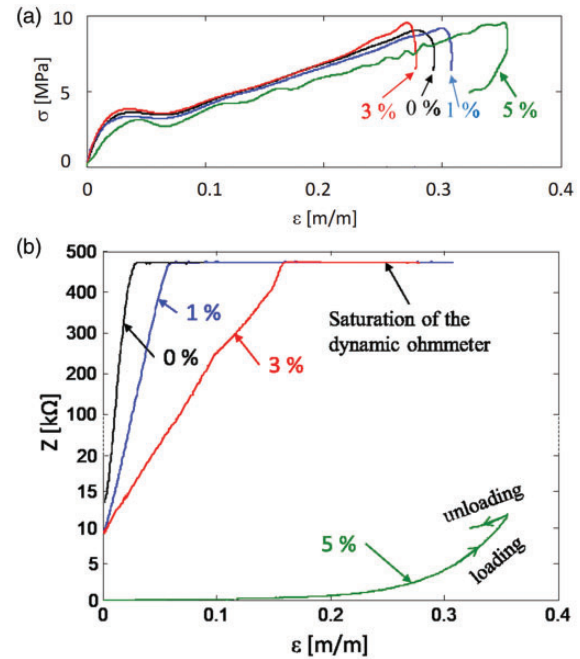


Figure 12. (a) Mechanical and (b) electrical behavior of the EPDM/MWCNT composites during SHPB compression.

fast, the values exceed the saturation of the electrical measurement device used (450 kΩ). So, the resistance could only be measured at the beginning of the dynamic compression.

As the MWCNT weight fraction decreases, the change in electrical resistance during the SHPB test is higher. This result is similar to the results observed during monotonic QS compression, given in the “Sensitivity of the composites under monotonic QS compression” section (Figure 11).

The changes in resistance during dynamic compression are attributed to reversible changes of the microstructure (movements of CNT) and damage inside the composite. The damage of the composite leads to an irreversible increase in the resistance and is the main piezoresistivity mechanism. Damage had also been observed by Heeder et al. on epoxy/MWCNT composite subjected to SHPB compression.² In their

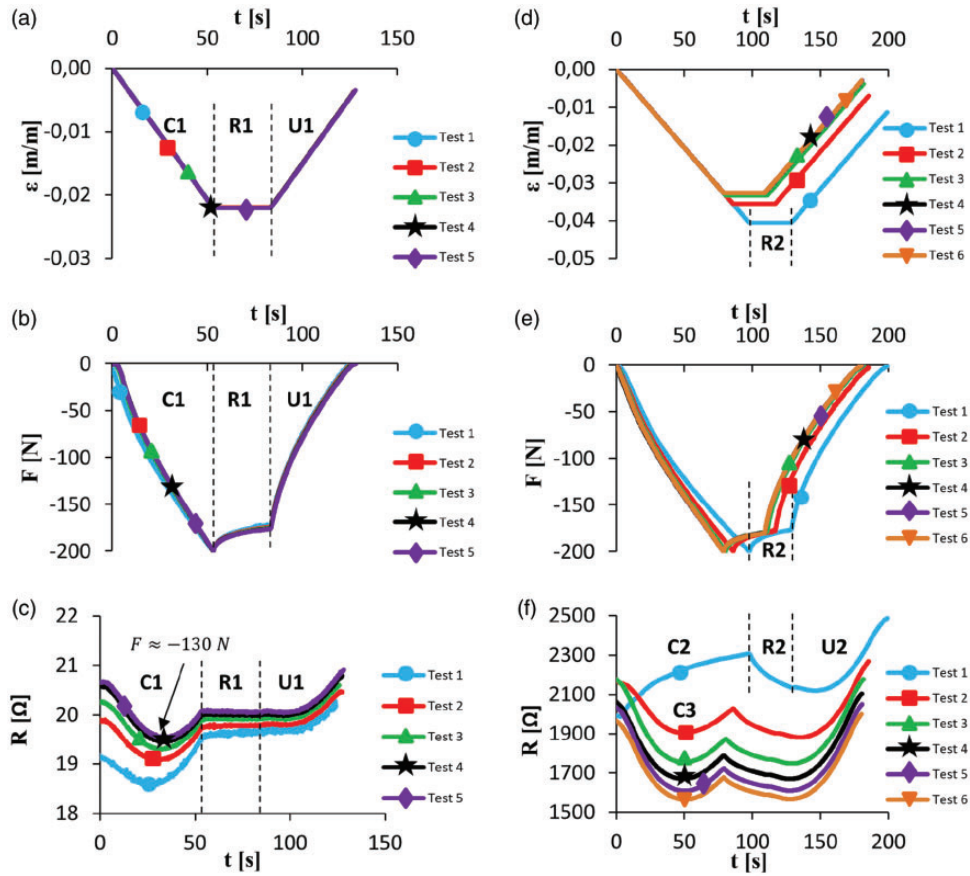


Figure 13. Change of force (a,d), strain (b,e) and electrical impedance (c,f) of an EPDM/5% MWCNT composite during consecutive QS compression cycles: (a–c) before SHPB experiment and (d–f) after SHPB experiment.

investigations, crack propagation was observed on the outer surface of their sample. In our case, damage is still assumed at this stage (as cracks could not be observed on the outer surface of our composite) and will be investigated in the following section.

Reversible changes of the resistance are seen as the resistance of the EPDM/5% MWCNT composite decreases slightly during the dynamic unloading.

During the dynamic tests, the compressive waves modify the particle networks in the sample. In the MWCNT 5%, the influence of the load is limited due to the high amount of particles. If the particle fraction is lowered under 3%, the polymer composites become more sensitive to the compressive load, showing high changes of their electrical response.

Damage induced by SHPB loading. To further assess the damage induced by dynamic loading, the QS tests defined in the “Characterization of the material piezoresistivity under quasi-static loading” section were applied again to the SHPB tested samples, after one week. Since similar trends were observed for the results of all materials, only those corresponding to

the EPDM/5% MWCNT composite are presented, as an example, in Figure 13. The compressive cycles applied to the EPDM/5% MWCNT before and after the SHPB test are represented in Figure 13(a) and (d), respectively. The first QS compression cycle was done one week after the end of the SHPB test. Each following QS compression cycle was separated by an interval of one day. The corresponding strains of the sample over the compressive cycles are plotted in Figure 13(b) and (e).

At the end of the SHPB test, the impedance of the EPDM/5% MWCNT composite was about 10 k Ω (Figure 12(b)). After one week of storage, the impedance decreased to 2 k Ω , indicating partial recovery of the composite. However, this value is still about 100 times higher than that of the raw sample (about 20 Ω).

In Figure 13, the left plots (a–c) and right plots (d–f) label QS tests, respectively, prior to and after the SHPB tests. Even though the trends of the impedance histories (c) and (f) are similar (except for test 1 in Figure 13(f)), it is worth highlighting a few features.

Similar impedance histories (Figure 13(c)) during all tests before the SHPB test are observed. During compression (label C1), the impedance decreases until a

minimum is reached (when the force is about -130 N), then increases until the force value is -200 N. During relaxation (label **R1**), the impedance is constant. During unloading (label **U1**), the impedance increases again.

After the SHPB experiment, the impedance increases during the compression of test 1 (label **C2** in Figure 13(f)). Micro-cracks may be initiated during high-speed compression. The application of a compression might enlarge these micro-cracks in the transversal axis, due to the lateral deformation by Poisson's effect. As a consequence, fewer contacts between conductive particles lead to increasing values of electrical impedance.

The resistance histories under compression of tests 2 to 6 displayed in Figure 13(f) (label **C3**) are similar to the ones shown in Figure 13(c). Moreover, the impedances values are shifted to lower values as seen in the offsets between consecutive tests. These are evidence that, although damaged, the material has recovered part of its initial electrical properties.

For all tests, the electrical impedance decreases during relaxation of plot 13(f) (label **R2**), unlike in the relaxation of plot 13(c) (label **R1**). Wang and Han¹⁸ found similar behavior for CNT-filled silicone rubber composites. It is attributed to a decrease in the distance between the CNT, because of the increase in their curvature and interactions with the elastomer matrix.

Figure 14 gives a comparison of the mechanical behavior before and after dynamic loading. Before and after SHPB tests, the Young's modulus (slope of the stress-strain curve at the origin) of this composite is, respectively, 50 MPa and 27.5 MPa, corresponding to a decrease of 45% after the SHPB test.

The amount of damage has not been directly quantified in this study. Nevertheless, it could be assessed by the decrease of the elastic modulus before and after the SHPB test, as in Figure 14. Damage could be also evaluated using 3D tomography technique allowing

highlighting the cavities, voids and cracks present in the specimen, before and after the dynamic test. A comparison between the two states should lead to the quantification of the damage amount.

Conclusions

The results of this work highlight the electro-mechanical behavior of composites made of an EPDM matrix, reinforced with CB (25 wt.%) and MWCNT (between 0 and 5 wt.%). Because of the presence of CB, the composites exhibit very low resistivity. When the weight fraction of MWCNT is over 3%, there is no dramatic change in the initial electrical conductivity of the composites. Adding MWCNT decreases the electrical impedance but lowers the sensitivity of the composites under quasi-static and dynamic compression. Reversible movements of CNT in the transverse direction of the compression increase the electrical resistance under quasi-static compression. These reversible movements are correlated with the good repeatability of the electrical response of all composites, observed during quasi-static cyclic compression. However, a shoulder effect was observed at the end of each compression and each unloading. The shoulder effect is more pronounced when the MWCNT weight fraction is high. Because of the effect of strain rate, the impedance of the composites is higher under dynamic compression than under quasi-static compression. A dramatic decrease in elastic modulus and increase in the electrical impedance after dynamic loading are indicators of damage induced by the dynamic loading.

Declaration of conflicting interests

The author(s) declared no potential conflicts of interest with respect to the research, authorship, and/or publication of this article.

Funding

The author(s) disclosed receipt of the following financial support for the research, authorship, and/or publication of this article: We thank the Region Centre Val De Loire for financial support during this research.

ORCID iD

André Langlet  <https://orcid.org/0000-0001-6159-623X>

References

1. Bokobza L. Multiwall carbon nanotube-filled natural rubber: electrical and mechanical properties. *EXPRESS Polym Lett* 2012; 6: 213–223.
2. Heeder N, Shukla A, Chalivendra V, et al. Sensitivity and dynamic electrical response of CNT-reinforced nanocomposites. *J Mater Sci* 2012; 47: 3808–3816.

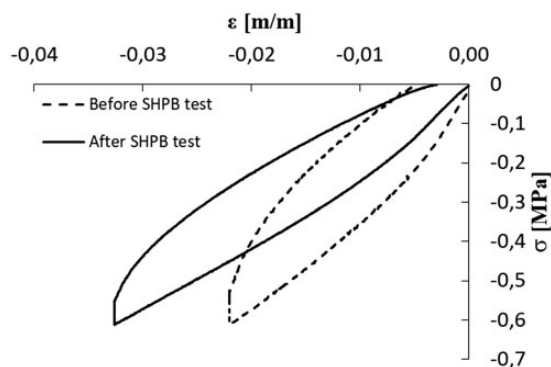


Figure 14. Stress-strain law for EPDM/5% MWCNT before and after SHPB tests.

3. Spinelli G, Lamberti P, Tucci V, et al. Experimental and theoretical study on piezoresistive properties of a structural resin reinforced with carbon nanotubes for strain sensing and damage monitoring. *Compos Part B Eng* 2018; 145: 90–99.
4. Spitalsky Z, Tasis D, Papagelis K, et al. Carbon nanotube-polymer composites: chemistry, processing, mechanical and electrical properties. *Prog Polym Sci* 2010; 35: 357–401.
5. Ciselli P, Lu L, Busfield JJC, et al. Piezoresistive polymer-composites based on EPDM and MWNTs for strain sensing applications. *e-Polymers* 2010; 14: 1–13.
6. Costa P, Ferreira A, Sencadas V, et al. Electro-mechanical properties of triblock copolymer styrene-butadiene-styrene/carbon nanotube composites for large deformation sensor applications. *Sensor Actuators A Phys* 2013; 201: 458–467.
7. Baltopoulos A, Polydorides N, Pambaguian L, et al. Exploiting carbon nanotube networks for damage assessment of fiber reinforced composites. *Compos Part B Eng* 2015; 76: 146–158.
8. Gao L, Chou TW, Thostenson ET, et al. In situ sensing of impact damage in epoxy/glass fiber composites using percolating carbon nanotube networks. *Carbon* 2011; 49: 3371–3391.
9. Huang YY and Teretjev EM. Dispersion of carbon nanotubes: mixing, sonication, stabilization, and composite properties. *Polymers* 2012; 4: 275–295.
10. Gong S and Zhu ZH. On the mechanism of piezoresistivity of carbon nanotube polymer composites. *Polymer* 2014; 55: 4136–4149.
11. Ku-Herrera JJ and Aviles F. Cyclic tension and compression piezoresistivity of carbon nanotube/vinyl ester composites in the elastic and plastic regimes. *Carbon* 2012; 50: 2592–2598.
12. Wang L and Han Y. Application of carbon nanotube filled silicone rubber composite in stress measurement during ramped loading with low compression speed. *Sensors Actuators A Phys* 2013; 201: 214–221.
13. Wang Y, Wang S, Li M, et al. Piezoresistive response of carbon nanotube composite film under laterally compressive strain. *Sensors Actuators A Phys* 2018; 273: 140–146.
14. Hao B, Mu L, Ma Q, et al. Stretchable and compressible strain sensor based on carbon nanotube foam/polymer nanocomposites with three-dimensional networks. *Compos Sci Technol* 2018; 163: 162–170.
15. Mitrakos V. *Design, development and characterisation of piezoresistive and capacitive polymeric pressure sensors for use in compression hosiery*. Master of Science Thesis, Heriot-Watt University, UK, 2014.
16. Zha JW, Li WK, Zhang J, et al. Influence of the second filler on the positive piezoresistance behavior of carbon nanotubes/silicone rubber composites. *Mater Lett* 2014; 118: 161–164.
17. Gary G and Zhao H. Dépouillement de l'essai aux barres de Hopkinson par une technique de calcul inverse. *J Phys IV France* 1994; IV: C8–89–C8–94.
18. Wang L and Han Y. Compressive relaxation of the stress and resistance for carbon nanotube filled silicone rubber composite. *Compos Part A Appl Sci Manuf* 2013; 47: 63–71.